Mechanical response of animal abdominal walls in vitro: Evaluation of the influence of a hernia defect and a repair with a mesh implanted intraperitoneally

Florence Podwojewski, Mélanie Ottenio, Philippe Beillas, Gaëtan Guerin, Frédéric Turquier, D. Mitton

PODWOJEWSKI, Florence ; OTTENIO, Mélanie ; BEILLAS, Philippe ; GUERIN, Gaëtan ; TURQUIER, Frédéric , 2013 , Mechanical response of animal abdominal walls in vitro: Evaluation of the influence of a hernia defect and a repair with a mesh implanted intraperitoneally , Journal of Biomechanics , 46 , 5 , ELSEVIER , pp. 882-889 , DOI: 10.1016/j.jbiomech.2012.09.014

Mechanical response of animal abdominal walls *in vitro*: Evaluation of the influence of a hernia defect and a repair with a mesh implanted intraperitoneally

F. Podwojewski[1,*], M. Otténio[1], P. Beillas[1], G. Guérin[2], F. Turquier[2], D. Mitton[1,*]

[1] Université de Lyon, F-69622, Lyon; IFSTTAR, LBMC, UMR_T9406, F-69675, Bron ; Université Lyon 1, Villeurbanne, France

[2] Covidien, Trévoux, France

[*] Corresponding author at: LBMC - Site Ifsttar Lyon-Bron, 25 Av. F. Mitterrand, Case 24, 69675 Bron Cedex, France. Tel.: +33 478656878; fax: +33 472376837

E-mail addresses: florence.podwojewski@ifsttar.fr (F. Podwojewski), david.mitton@ifsttar.fr (D. Mitton).

Word count: 3535 words

ABSTRACT

Better mechanical knowledge of the abdominal wall is requested to further develop and validate numerical models. The aim of this study was to characterize the passive behaviour of the abdominal wall under three configurations: intact, after creating a defect simulating an incisional hernia, and after a repair with a mesh implanted intraperitonally. For each configuration, controlled boundary conditions were applied (air pressure and then contact loading) to the abdominal wall. 3D Local strain fields were determined by digital image correlation. Local strains measured on the internal and external surfaces of the intact abdominal wall showed different patterns. The air pressure and the force applied to the abdominal wall during contact loading were measured and used to determine stiffness. The presence of a defect resulted in a significant decrease of the global stiffness compared to the intact abdominal wall (about 25%). In addition, the presence of the mesh enabled to restore the stiffness to values that were not significantly different from those of the intact wall. These results suggest that intraperitoneal mesh seems to restore the global biomechanics of the abdomen.

Keywords: Biomechanics, mesh repair, digital image correlation, pressure, contact loading.

1. Introduction

Treatment of incisional hernias is a common surgical procedure (Cobb et al., 2003). The laparoscopic repair with mesh implantation improves the treatment of incisional hernia by reducing the rate of recurrence and risk of wound complication (Cobb et al., 2005a). The use of composite mesh, that limits adhesions with abdominal organs, makes the laparoscopic repair easier by putting the mesh in the intraperitoneal location (Cobb et al., 2003). However, problems of recurrence can still happen. Problems of restriction of the abdominal wall mobility or pains may also occur to patients (McLanahan et al., 1997; Müller et al., 1998). Studies on the interaction of mesh with the abdominal wall have been performed. Factors identified as possible causes of recurrence include the size of the implanted mesh compared to the size of the defect (the overlap), and the method of mesh fixation (Binnebösel et al., 2007; Schwab et al., 2008). It has also been suggested that the mesh structure should be improved in order to have similar biomechanical behaviour to the abdominal wall to reduce discomforts (Konerding et al., 2011a; Hernández et al., 2011).

Numerical models could be useful to assess the influence of a mesh on the behaviour of the abdominal wall. In particular, such models could be used to evaluate the possible effects of mesh design changes or implantation procedures very early in the design process. However, experimental data on the mechanical response of the abdominal wall are a prerequisite to develop models. Hernández et al. (2011) conducted uniaxial tensile tests on the flat abdominal muscles of rabbits in order to characterize the passive behaviour of the abdominal wall and develop a numerical model of a healthy and a partially herniated repaired abdominal wall of rabbit (Hernández-Gascón et al., 2011). Förstemann et al. (2011) performed uniaxial tensile tests on the linea alba to develop an analytical model of the abdominal wall. While these studies can provide useful data to help in building a model, they cannot be used to evaluate or validate the performance of a whole abdominal wall model subjected to mechanical load.

Thus, Konerding et al. (2011a) performed a human cadaver study to validate the model proposed by Förstemann et al. (2011).

Song et al. (2006) and Szymczak et al. (2012) studied the complete human abdominal wall response respectively to pressure during a laparoscopic surgery and during different physical exercises. While such studies provide a useful starting point for the validation of model, it only included data on the response of the external surface of the intact human abdominal wall . This is an important limitation for the validation of a model, whose purpose is to study the interaction of the mesh with the wall when implanted on the internal surface. No study comparing the behaviour of the external wall (skin side) and the internal wall (peritoneal side) could be found in the literature.

Furthermore, many studies provide experimental results on the mechanical properties of the complete abdominal wall (Song et al., 2006; Konerding et al., 2011a; Junge et al., 2001) and its components (Hernández et al., 2011; Förstemann et al., 2011; Rath et al., 1996, Hollinsky et al., 2007), or on the characterization of meshes only (Junge et al., 2001; Hernández-Gascón et al., 2011). However, only a few studies were found regarding the mechanical response of the abdominal wall with an implanted mesh, and how it may differ from the response of a healthy wall. Müller et al. (1998) studied the difference of abdominal wall mobility between a healthy control group and a group of patients with incisional hernia, who was treated by mesh implantation. Hernández-Gascón et al. (2011) observed the mechanical response of intact abdominal wall and abdominal wall that was repaired using different meshes on rabbits. This study was performed on small animals and only the lateral part of the abdominal wall was considered. Also, samples were characterized by uniaxial test that do not reproduce the physiological loading conditions of the abdominal wall. To the authors' knowledge, no studies compared the behaviour of a same intact abdominal wall, and then implanted with a mesh.

Therefore, the current study focused on the anterolateral abdominal wall, where incisional hernias may occur. The objective of this work was to study the response of a same abdominal wall under three different states: intact, with a hernia defect, and repaired. Particular attention was paid to study simultaneously the internal and external surfaces. Boundary and loading conditions were defined to ensure reproducibility and control.

2. Materials and methods

2.1 Specimen & preparation

Anterolateral abdominal walls of six female pigs, aged 4 to 5 months and weighing about 45 kg, were used for the current study. The abdominal walls were removed from the animals less than 30 minutes after euthanasia at the VetAgro Sup, Veterinary Campus of Lyon (Marcy l'Etoile, France), and then kept frozen at -20°C until testing. The abdominal walls were cut along the xiphoid process and the costal margins and along the pubic bones and the iliac crests. The lateral incisions were done between the iliac spines and the lower part of the rib cage. Thus the abdominal wall had a triangular shape (Fig. 1). All the layers were preserved: muscles, aponeuroses, adipose tissue, skin and peritoneum. The abdominal walls were thawed at room temperature 16 hours before the test. Just before testing, the external surface of the abdominal wall was shaved. The thickness of each abdominal wall was also measured (Fig. 1) and their average thickness is reported in Table 1. The specimens were sprayed with saline solution to enable their hydration.

2.2 Experimental setup

First, the abdominal wall was placed on a hemispherical support (diameter of 9 cm) in order to induce a curvature. Then, it was put on an aluminum plate with a triangular hole exposing the anterolateral abdominal wall. A rubber sheet with the same hole was added to cover the

section of the abdominal wall outside the hole. This sheet was clamped using custom designed clamps positioned all around the hole (Fig.2a). As the abdominal wall thickness was not constant over its circumference, the clamps were adjusted to provide adequate tightening in over the whole circumference and prevent local sliding during loading. The abdominal wall was not removed from this fixture until the very end of the experiment.

Then, the abdominal wall was positioned on a custom designed aluminium table mounted on a testing machine (INSTRON 8802, High Wycombe, England) (Fig. 2b). The external face of the wall was directed downwards, leading to a natural curvature due to gravity.

Physiologically, the abdominal wall can be loaded by contact of the hollow organs or by pressure in case of laparoscopic surgery. So, during the experiment, the abdominal wall was submitted to two mechanical loading cases: contact and air pressure.

First, the air pressure was applied on the internal surface (Fig. 3a). A Plexiglas plate was mounted on the top of the aluminium plate in order to create a closed cavity. The Plexiglas plate was transparent, allowing to observe the internal abdominal wall. Compressed air and a manual valve were used to control the pressure in the cavity. At a laparoscopic pressure of 12 mmHg, a smaller displacement of the abdominal wall than the one measured by Song et al. (2006) was observed due to strong boundary conditions. So, the pressure was increased until it reaches 50 mmHg, which is in the physiological range of intra-abdominal pressure (Cobb et al., 2005b). Then, it was let to return to atmospheric pressure by opening the valve. The pressure loading cycle was repeated six times. The first 5 cycles enabled to precondition the wall in order to reach a steady state, limiting variability to assess various conditions. Only the sixth cycle of pressurization was used for the data analysis.

Then, a contact loading was applied to the internal side using a rigid sphere, to better control the loading conditions for further numerical model (Fig. 3b). After the pressurization test, the Plexiglas plate was removed and the abdominal wall was loaded directly by the rigid

Plexiglas sphere (12 cm in diameter) fixed to the actuator of the testing machine. First, the sphere was moved to get in contact with the abdominal wall. Then, the specimen was preconditioned with 5 cycles of 20 mm amplitude at a frequency of 0.5 Hz, close to the respiratory frequency. A displacement of 35 mm, which is in the range of physiological displacement of the abdominal wall (Klinge et al., 1998), was finally applied at a velocity of 80 mm per minute. The velocity was slow enough to characterize the quasi-static response and also led to a short duration of test that limit the quite long duration of all the protocol.

An incision was made in the middle of the linea alba over a length of 5 cm, which is the size of a medium incisional hernia. The skin was kept intact. The incision was filled with Vaseline and covered with a latex film to avoid air leaks below the skin during pressure loading. The incised abdominal wall was re-loaded. Then a surgical repair was performed using a 10*15 cm^2 Parietex® Composite mesh, centred on the defect and fixed on the wall with 20 tackers (AbsorbaTack®). The tackers were located at one centimetre of the border of the implant and spaced apart 2 cm. A plastic film (15*20 cm^2, thickness 10µm) was put on the mesh to avoid air infiltrations between the implant and the peritoneum. Finally the repaired abdominal wall was loaded in the same conditions.

In summary, the abdominal walls were loaded consecutively by pressure and contact in the three following states:

- intact abdominal wall,
- incised abdominal wall (after creating a defect simulating an incisional hernia),
- repaired abdominal wall (finally after surgical repair by mesh implantation).

2.3 Testing duration influence on an intact abdominal wall behaviour

Beforehand, a healthy abdominal wall was tested to assess the effect of time and of the loading sequence on the abdominal wall response. An abdominal wall was subjected to the protocol twice within 4 hours, by switching the different loading cases (pressure, contact and pressure loading again). Between the two series of tests, the specimen was covered with moist gauzes.

2.4 Measurements

The pressure and the force applied by the sphere to the abdominal wall were measured by a 7 bar ENTRAN EPX-N02 pressure sensor and a 1000 N INSTRON force sensor (accuracy 0.5%), respectively.

Four synchronized SA3 PHOTRON black and white video cameras (Tokyo, Japan) were used to record videos of the abdominal wall during the deformation. Two cameras equipped with 35 mm Zeiss lenses (Oberkochen, Germany) were set on the internal surface, and the two others (equipped with 24-70mm Sigma lenses (Tokyo, Japan) in 24 mm position) were set on the external surface. The resolution of the cameras was 1024 by 1024 pixels, which led to approximately 3 pixels per mm in the area of interest. The acquisition frequency was 10 frames per second.

Before testing, the two faces of the abdominal wall were covered with white make-up to make the background uniform. Then a random speckle pattern was applied with a black paint spray . The speckle enabled to determine 3D local displacement and 3D strain fields by digital image correlation using the VIC3D® stereo-correlation software (Correlated Solution, South Carolina, USA).

2.5 Data analysis

For the contact loading case, the force versus displacement curves were plotted for the last (6^{th}) loading cycle, and a stiffness in N/mm was worked on. This stiffness was calculated as the slope of the curve determined by linear regression between 26 and 30 mm of displacement (Fig. 4). This interval of displacement defined a common quasi linear area for all the tested abdominal walls. The relative differences of stiffness were calculated between two states, $\Delta_{state_1-state_2} = \frac{S_{state_2} - S_{state_1}}{S_{state_1}} \times 100$, where S is the stiffness.

The displacement and strain fields were obtained by stereo correlation for all configurations and for both loading cases on the external wall surface. The strain fields could only be computed on the intact internal wall surface for pressure loading because the Plexiglas sphere hid the internal wall surface during the test. An average strain value was calculated in the central area of the abdominal wall (~ 70mm*105mm between the nipples) from the Lagrange strain values computed by Vic 3D in first principal direction (E1) (Fig. 5).Average strains along longitudinal (linea alba) and transverse lines of the external abdominal wall surface were also calculated for the pressure loading case.

2.6 Statistical analysis

A statistical analysis was performed in order to assess the influence of the state (intact, incised, and repaired) of the abdominal wall on its mechanical response. A Wilcoxon non-parametric test (Wilcoxon, 1945) for paired samples was used. A value of $p < 0.05$ was selected to indicate statistical significance. Parameters studied are the stiffness and the average strain. Statistical analysis was performed using Unistat® software (London, England).

3. Results

3.1 Testing duration influence on an intact abdominal wall behaviour

For both mechanical loading, the mechanical response of the abdominal wall was found to be non-linear, with a toe zone followed by a more linear zone . The unloading curve did not overlap with the loading curve. As an example, the force-displacement curves for contact loading are given Fig. 4. A similar mechanical response was obtained whatever the time of test for the pressure and the contact loading, with respectively difference of stiffness of about 5% and 10%.

3.2 Relation between internal and external surface strains in the intact abdominal wall

The strain fields of the internal and the external abdominal wall surfaces exhibited different patterns as illustrated on Fig. 5. The location of the maximum strain on the internal surface did not match the location of the maximum strain on the external surface. On the internal surface, a region of greater strain near the long edge was observed. On the external surface, there was less strain near the edges and especially at the three corners of the triangle.

Table 1 displays the mean value and the standard deviation of the local strains in the central area for the internal and external surfaces for the pressure loading case at 50 mmHg. The average strain in the central area of the external surface (13.7 (2.1) %) was almost 2.6 higher than the mean strain of the internal surface (5.3 (0.7) %), with variation of 23.3%.

3.3 Influence of a defect and of mesh repair on the behaviour of the abdominal wall

The curves of the contact loading case for the three studied states are displayed on Fig. 6. Mean stiffness calculated for each state are presented in Fig. 7. The difference of stiffness between intact walls and incised walls was statistically significant ($p = 0.03$). However, the stiffness obtained for intact and repaired states were similar ($p = 0.43$). Relative differences between the abdominal walls states are summarized Table 2. The stiffness of the incised cases

was lower by about 25% than the stiffness of intact cases. There was a smaller relative difference of stiffness between intact and repaired walls; the stiffness of intact cases was 6% greater than the stiffness of repaired cases.

The mean strains values computed in the central area for the external surfaces of the abdominal wall for each configuration and loading case are displayed in Table 3. For both pressure and contact loading cases, the defect had a significant effect on the strain of the abdominal wall ($p = 0.03$). The defect increased the average strain of about 74% and 35% respectively for the pressure and contact loading. For both loading cases , significant differences of strains were found between incised and repaired states ($p = 0.03$). For the pressure loading case, significant differences of strains were found betweenintact and repaired states ($p = 0.03$) whereas no significant differences were found for the contact loading case ($p = 0.81$). More elongation was observed in the longitudinal direction than in the transverse direction for each state (e.g. for the repaired state: 15.9 (3.0) % and 15.3 (2.8) % respectively) The defect doubled the average strains along the two directions. No differences were found between incised and repaired states.

4. Discussion

In this study, an experimental protocol was developed to characterize the mechanical response of animal passive abdominal wall in three states (intact, incised and repaired) and for two loading cases (increased air pressure similar to a laparoscopic procedure and contact loading). The test of an intact abdominal wall on a day showed that the evolution of the mechanical response of a wall is low (relative difference of 10% for the stiffness). Thus, the duration of the test on a same abdominal wall has limited influence on its behaviour. So, it is expected that differences observed for each configuration can be attributed to the change of state and not to the duration of the protocol.

This study was conducted on porcine abdominal walls. An animal model was used to develop the protocol since the anatomical samples were easier to access than those of human. Pig was chosen, because the dimensions of its abdominal wall are close to those of human. Swine are also often used in biomedical research since they have large anatomical and physiological similarities with humans (Swindle et al., 1998). In addition, the experiments on porcine abdominal walls allowed us to validate the repeatability of our protocol. For six specimens with small inter-individual variability (pigs of same weight, about 45kg, and of same age, between 4-5 months) and with very constrained testing boundary conditions, relatively small variability of the stiffness data was observed, with variations in the order of 12.3% for the intact state, 16.5% for the incised state, and 6 % for the repaired state.

This study also shows the influence of a defect and a mesh repair on the behaviour of the abdominal wall. The defect decreased the stiffness of the intact abdominal wall by 25% on average and increased the average strain of the abdominal wall by about 74% and 35% respectively for the pressure and contact loading cases. The presence of the mesh in immediate postoperative configuration on an incised abdominal wall enabled to restore the stiffness to values that were not significantly different from those of an intact wall. Other studies interested in the repaired abdominal wall, but when the mesh is integrated. Konerding et al. (2011b) compared the response of different types of meshes that are integrated to the abdominal wall without referring to intact abdominal wall behaviour. This is not the case for the study of Hernández-Gascón et al. (2012) that assessed the response of the repaired abdominal wall and compared it to the response of intact abdominal wall. However, the response was obtained by uniaxial test.

For the first time, this study provides data on the strain fields of the abdominal wall for the internal and external surfaces. Szymczak et al. (2012) highlight the interest of studying the internal abdominal wall surface since it is where incisional hernias occur. However, as they

performed *in vivo* experiments, they only considered the external abdominal surface. The mean strains computed on the external surface of the abdominal wall were found to be 2.6 times greater than those computed on the internal surface of the abdominal wall. For *in vivo* study, only the external surface of the abdominal wall can be measured. It is unclear if the mean ratio found between internal and external strains can be applied because of the difference of boundary conditions and of the muscular activity. Also, specimen to specimen variations on this ratio were relatively high (23.3 %). This suggests that relatively large uncertainties would be associated with the estimation of internal strains solely based on external strains.

.

Regarding the present study, some limitations can be mentioned. The effect of freezing was not considered however the literature is often contradictory on the effect of freezing of soft tissues (Van Ee et al., 2000; Clavert et al., 2001; Rubod et al., 2007). During harvesting, there was no opportunity to measure the curvature of the abdominal wall and the shortening of tissues. Thus, the initial curvature and tension could not be reproduced *in vitro*. The initial tension and boundary conditions were not representative of physiological conditions. Perspectives of this study are to approach the physiological conditions with *in vivo* experiments. The anisotropy of the strain was assessed in this study but the analysis is limited by the shape of the current device which is not symmetric. However, these findings correspond with the studies analysing the surface deformation of the *in vivo* human abdominal wall (Song et al., 2006 and Szymczak et al., 2012). Boundary conditions were well controlled in order to develop a numerical model. Due to the strong boundary conditions, the results of stereo-correlation showed artefact near the edges for the pressure loading case. So, the strains

patterns analysis was restricted to the central part of the abdominal wall limited by the nipples.

The main results of this study regarding the stiffness variations between states are currently used to test the validity of numerical models of a porcine abdominal wall. In the future, the same methodology will be used to characterize the passive response of human abdominal walls.

Acknowledgements

This study was partly funded by Covidien Company.

Conflict of interest statement

This study was partly funded by Covidien Company. G. Guérin and F. Turquier are employees of Covidien France.

References

Binnebösel, M., Rosch, R., Junge, K., Flanagan, T.C., Schwab, R., Schumpelick, V., Klinge, U., 2007. Biomechanical analyses of overlap and mesh dislocation in an incisional hernia model in vitro. Surgery 142 (3), 365-371.

Clavert, P., Kempf, J.F., Bonnomet, F., Boutemy, P., Marcelin, L., Kahn, J.L., 2001. Effects of freezing/thawing on the biomechanical properties of human tendons. Surgical and Radiologic Anatomy 23 (4), 259-262.

Cobb, W.S., Harris, J.B., Lokey, J.S., McGill, E.S., Klove, K.V., 2003. Incisional herniorrhaphy with intraperitoneal composite mesh: a report of 95 cases. American Surgeon 69 (9), 784-787.

Cobb, W.S., Kercher, K.W., Heniford, B.T., 2005a. Laparoscopic repair of incisional hernias. Surgical Clinics of North America 85 (1), 91-103.

Cobb, W.S., Burns J.M., Kercher, K.W., Matthews, B.D., James Horton, H., Todd Heniford, B., 2005b. Normal intraabdominal pressure in healthy adults. Journal of Surgical Research 129 (2), 231-235.

Förstemann, T., Trzewik, J., Holste, J., Batke, B., Konerding, M.A., Wolloscheck, T., Hartung, C., 2011. Forces and deformations of the abdominal wall – a mechanical and geometrical approach to the linea alba. Journal of Biomechanics 44 (4), 600-606.

Hernández, B., Peña, E., Pascual, G., Rodríguez, M., Calvo, B., Doblaré, M., Bellón, J.M., 2011. Mechanical and histological characterization of the abdominal muscle. A previous step to modelling hernia surgery. Journal of the Mechanical Behavior of Biomedical Materials 4 (3), 392-404.

Hernández-Gascón, B., Peña, E., Melero, H., Pascual, G., Doblaré, M., Ginebra, M.P., Bellón, J.M., Calvo, B., 2011. Mechanical behaviour of synthetic surgical meshes: Finite element simulation of the herniated abdominal wall. Acta Biomaterialia 7 (11), 3905-3913.

Hernández-Gascón, B., Peña, E., Pascual, G., Rodríguez, M., Bellón, J.M., Calvo, B., 2012. Long-term anisotropic mechanical response of surgical meshes used to repair abdominal wall defects. Journal of the Mechanical Behavior of Biomedical Materials 5 (1), 257-271.

Hollinsky, C., Sandberg, S., 2007. Measurement of the tensile strength of the ventral abdominal wall in comparison with scar tissue. Clinical Biomechanics 22 (1), 88–92.

Junge ,K., Klinge, U., Prescher, A., Giboni, P., Niewiera, M., Schumpelick, V., 2001. Elasticity of the anterior abdominal wall and impact for reparation of incisional hernias using mesh implants. Hernia 5 (3), 113-118.

Konerding, M.A., Bohn, M., Wolloscheck, T., Batke, B., Holste, J.L., Wohlert, S., Trzewik, J., Förstemann, T., Hartung, C., 2011a. Maximum forces acting on the abdominal wall: Experimental validation of a theoretical modeling in a human cadaver study. Medical Engineering & Physics 33 (6), 789-792.

Konerding, M.A., Chantereau, P., Delventhal, V., Holste, J.L., Ackermann, M., 2011b. Biomechanical and histological evaluation of abdominal wall compliance with intraperitoneal onlay mesh implants in rabbits: A comparison of six different state-of-the-art meshes. Medical Engineering & Physics, doi:10.1016/j.medengphy.2011.09.022.

McLanahan, D., King, L.T., Weems, C., Novotney, M., Gibson, K., 1997. Retrorectus prosthetic mesh repair of midline abdominal hernia. American Journal of Surgery 173 (5), 445-449.

Müller, M., Klinge, U., Conze, J., Schumpelick, V., 1998. Abdominal wall compliance after Marlex mesh implantation for incisional hernia repair. Hernia 2, 113-117.

Rath, A.M., Attali, P., Dumas, J.L., Goldlust, D., Zhang, J., Chevrel, J.P., 1996. The abdominal linea alba: an anatomo-radiologic and biomechanical study. Surgical Radiologic Anatomy 18 (4), 281-288.

383 Rubod, C., Boukerrou, M., Brieu, M., Dubois, P., Cosson, M., 2007. Biomechanical
384 properties of vaginal tissue. Part 1: new experimental protocol. Journal of Urology 178 (1),
385 320-325.
386 Schwab, R., Schumacher, O., Junge, K., Binnebösel, M., Klinge, U., Becker, H.P.,
387 Schumpelick, V., 2008. Biomechanical analyses of mesh fixation in TAPP and TEP hernia
388 repair. Surgical Endoscopy 22 (3), 731-738.
389 Song, C., Alijani, A., Frank, T., Hanna, G., Cuschieri, A., 2006. Elasticity of the living
390 abdominal wall in laparoscopic surgery. Journal of Biomechanics 39 (3), 587-591.
391 Swindle, M.M., Smith A.C., 1998. Comparative anatomy and physiology of the pig.
392 Scandinavian Journal of Laboratory Animal Science 25 (1), 11-21.
393 Szymczak, C., Lubowiecka I., Tomaszewska, A., Smietański, M., 2012. Investigation of
394 abdomen surface deformation due to life excitation: Implications for implant selection and
395 orientation in laparoscopic ventral hernia repair. Clinical Biomechanics 27 (2), 105-110.
396 Van Ee, C.A., Chasse, A.L., Myers, B.S., 2000. Quantifying skeletal muscle properties in
397 cadaveric test specimens: effects of mechanical loading, postmortem time, and freezer
398 storage. Journal of Biomechanical Engineering 122 (1), 9-14.
399
400
401

Figure legends:

Fig. 1. Part of the abdominal wall removed from pigs for the tests: (a) The incisions were made along the dotted line. (b) The thickness of the abdominal wall was measured in several points (A to H).

Fig. 2. Experimental device: (a) Tightening of the abdominal wall between an aluminium plate and a rubber sheet with clamps screwed in the plate. (b) Positioning of the abdominal wall on the table of the testing machine and arrangement of the cameras.

Fig. 3. Loading mechanisms: (a) Pressure loading, (b) Contact loading

Fig. 4. Calculation of the stiffness (N/mm) for the contact loading case. The stiffness was computed in the linear region of the curve between 26 and 30 mm of displacement.

Fig. 5. Lagrange first principal strain fields of the internal (a) and external (b) surfaces of an abdominal wall (sternum side at the top of the figure) subjected to a 50mmHg air pressure. Average strains were calculated in the central area inside the dotted lines.

Fig. 6. Displacement- Force curves for the contact loading for the three states. Error bars: Standard deviation

Fig. 7. Mean stiffness calculated for the contact loading case for each abdominal wall state: intact, incised and repaired (n=6). Error-bars: standard deviation.

Table 1. Mean Lagrange first principal strains E1 in % calculated for the internal and external surfaces of each abdominal wall for the pressure loading case at 50 mmHg.

Table 2. Relative difference of stiffness between the abdominal wall states for the contact loading case.

Table 3. Mean Lagrange first principal strains E1 in % calculated for the external surface of each abdominal wall for the pressure at 50mmHg and for the contact at 165N.

Fig. 1.

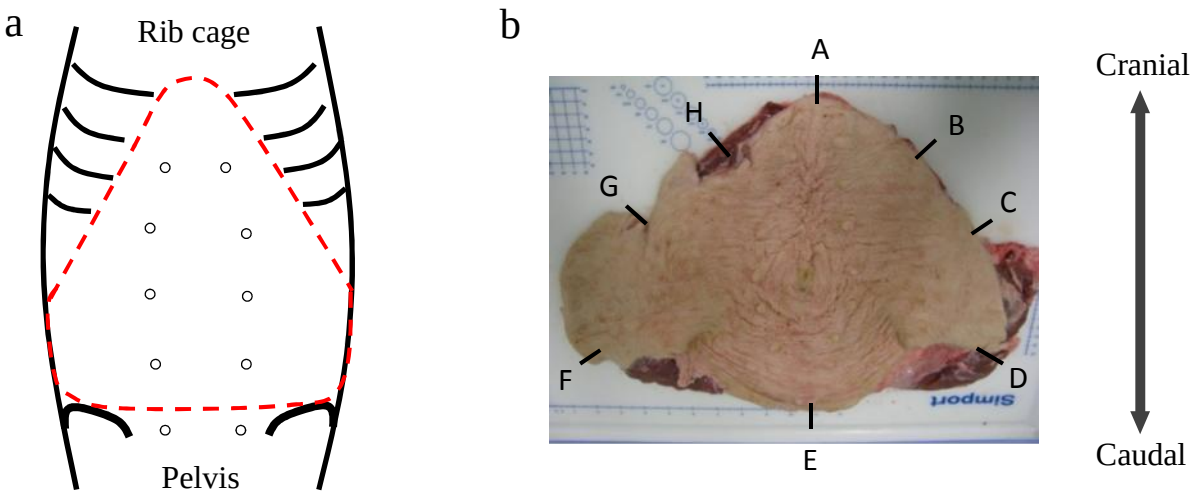

Fig. 2.

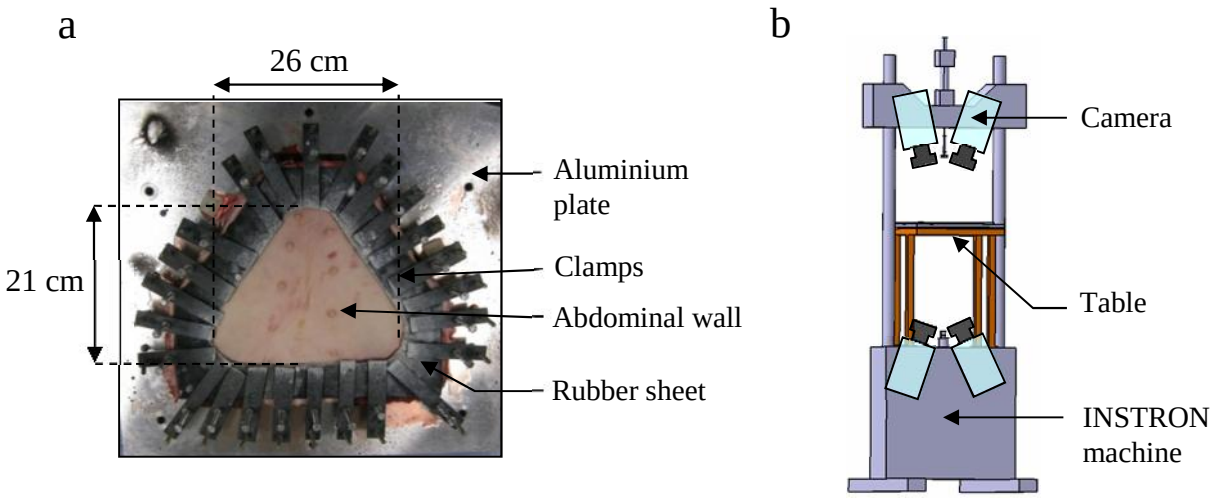
a
26 cm
21 cm
Aluminium plate
Clamps
Abdominal wall
Rubber sheet
b
Camera
Table
INSTRON machine

Fig. 3.

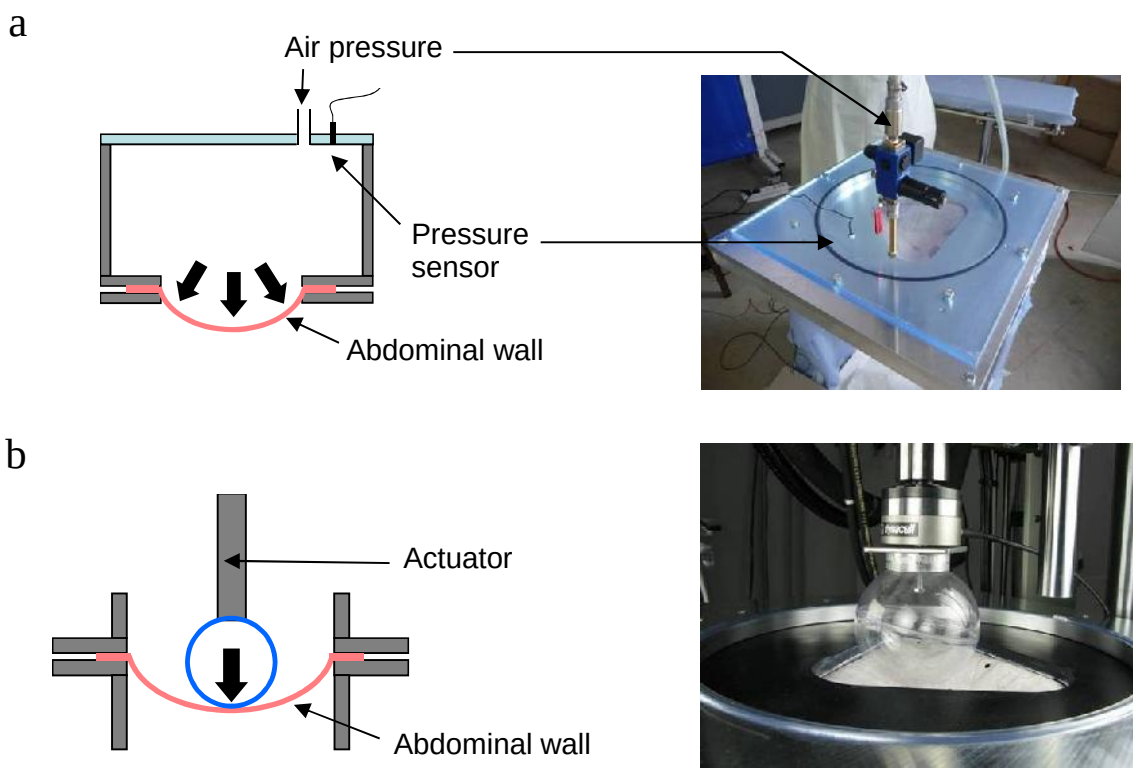
a
Air pressure
Pressure sensor
Abdominal wall
b
Actuator
Abdominal wall

Fig. 4.

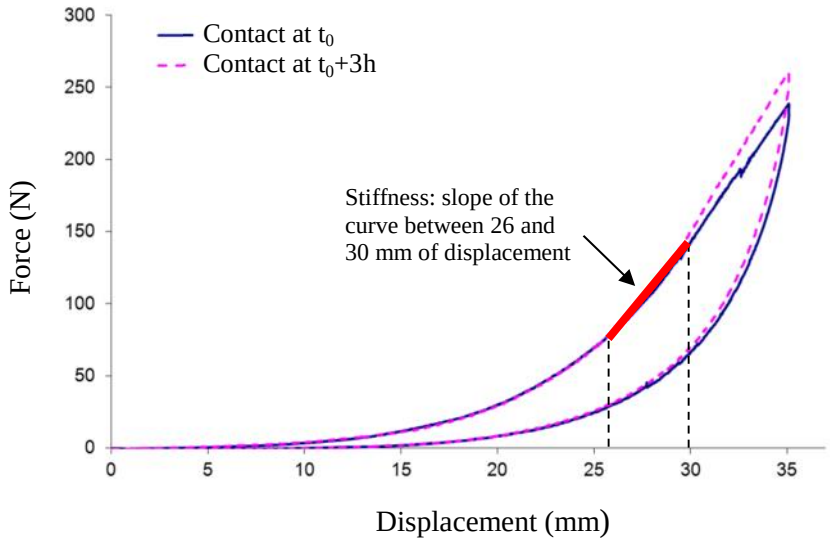
Contact at t_0
Contact at t_0+3h
Stiffness: slope of the curve between 26 and 30 mm of displacement
Force (N)
Displacement (mm)
300
250
200
150
100
50
0
0
5
10
15
20
25
30
35

Fig. 5.

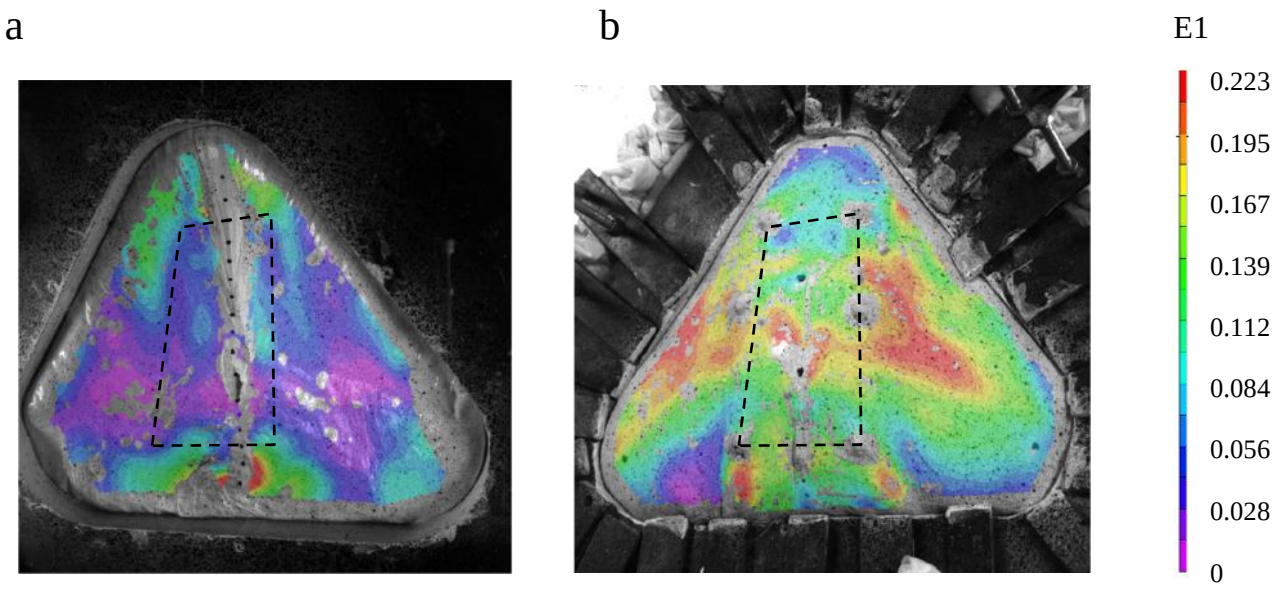

Fig. 6.

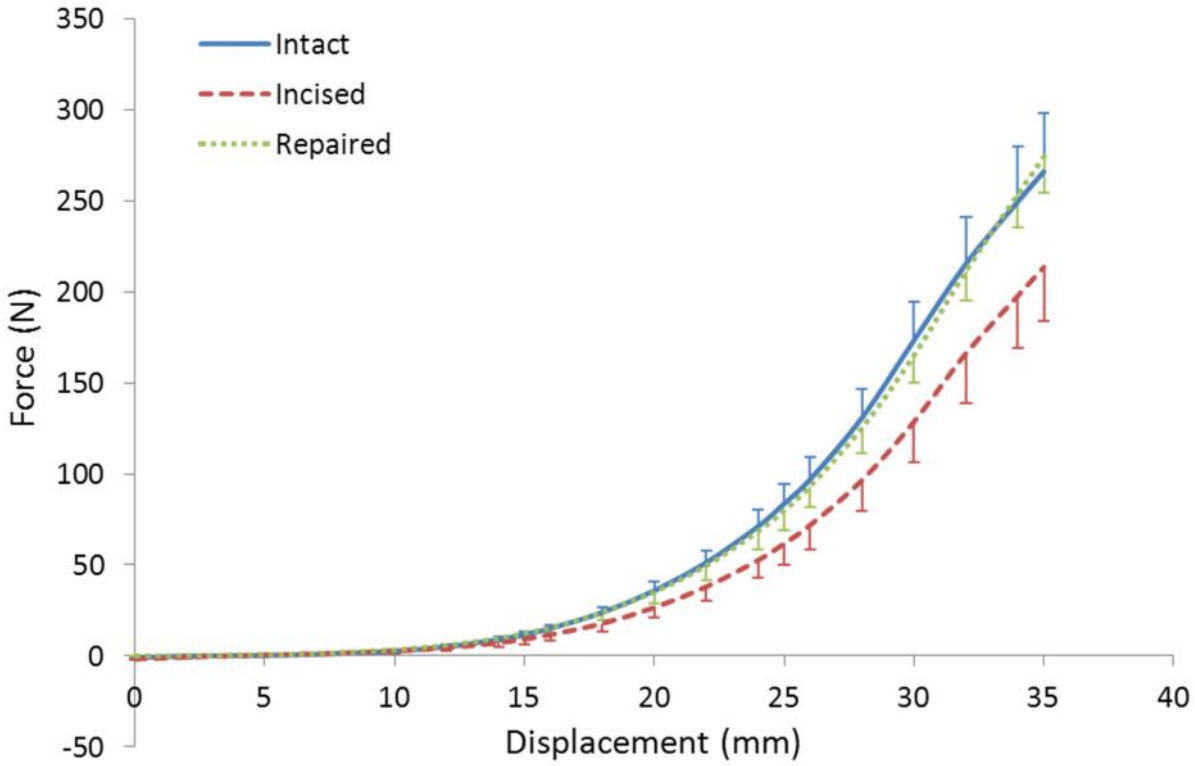
Intact
Incised
Repaired
Force (N)
Displacement (mm)
350
300
250
200
150
100
50
0
-50
0
5
10
15
20
25
30
35
40

Fig. 7.

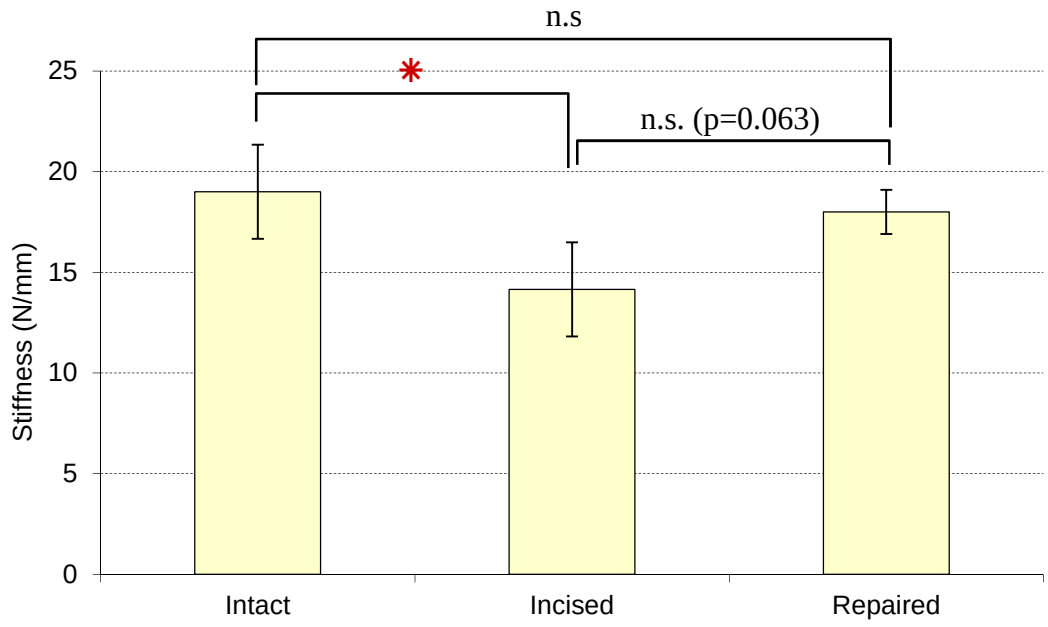

* : $p < 0.05$
n.s: not significant

Table 1

	Thickness (mm)	E1 (%) Internal surface	E1 (%) External surface	Ratio E1 Ext. / E1 Int.
Wall 1	28	4.4	13.7	3.1
Wall 2	25	4.5	17.3	3.8
Wall 3	29	5.6	13.4	2.4
Wall 4	27	5.0	10.8	2.1
Wall 5	30	6.6	14.9	2.3
Wall 6	30	5.5	12.0	2.2
Mean	*28*	*5.3*	*13.7*	*2.6*
SD	*1.7*	*0.7*	*2.1*	*0.6*

Table 2

	$\Delta_{\text{Intact-Incised}}$ (%)	$\Delta_{\text{Intact-Repaired}}$ (%)	$\Delta_{\text{Incised-Repaired}}$ (%)
Wall 1	-32	-4	42
Wall 2	-26	3	39
Wall 3	-17	-24	-9
Wall 4	-10	23	37
Wall 5	-43	-12	55
Wall 6	-21	-7	18
Mean	*-25*	*-4*	*30*

Table 3

	Mean strain E1 (%) Pressure (P=50 mmHg) – External surface			Mean strain E1 (%) Contact (F=165N) – External surface		
	Intact	Incised	Repaired	Intact	Incised	Repaired
Wall 1	13.7	25.9	20.7	11.0	14.4	13.2
Wall 2	17.3	22.4	20.2	23.0	26.9	19.8
Wall 3	13.4	18.3	17.7	15.5	19.2	15.3
Wall 4	10.8	24.6	15.3	12.5	19.1	14.4
Wall 5	14.9	23.3	22.2	15.2	21.1	15.0
Wall 6	12.0	28.7	21.6	9.8	17.1	12.6
Mean	*13.7*	*23.9*	*19.6*	*14.5*	*19.6*	*15.0*
SD	*2.1*	*3.2*	*2.4*	*4.3*	*3.9*	*2.3*